Original Article

Tomosyn Is Expressed in β-Cells and Negatively Regulates Insulin Exocytosis

Wei Zhang,[1] Lena Lilja,[2] Slavena A. Mandic,[2] Jesper Gromada,[3,4] Kamille Smidt,[3] Juliette Janson,[2] Yoshimi Takai,[5] Christina Bark,[2] Per-Olof Berggren,[2] and Björn Meister[1]

Tomosyn, a syntaxin-binding protein, is capable of dissociating mammalian homolog of the *Caenorhabditis elegans unc-18* gene from syntaxin and is involved in the regulation of exocytosis. We have investigated the expression, cellular localization, and functional role of tomosyn in pancreatic β-cells. Western blotting revealed a 130-kDa protein corresponding to tomosyn in insulin-secreting β-cell lines. RT-PCR amplification showed that b-, m-, and s-tomosyn isoform mRNAs are expressed in β-cell lines and rat pancreatic islets. Immunohistochemistry revealed punctate tomosyn immunoreactivity in the cytoplasm of insulin-, glucagon-, pancreatic polypeptide–, and somatostatin-containing islet cells. Syntaxin 1 coimmunoprecipitated with tomosyn in extracts of insulin-secreting cells. Overexpression of m-tomosyn in mouse β-cells significantly decreased exocytosis, whereas inhibition of tomosyn expression by small interfering RNA increased exocytosis. Hence, in the pancreatic β-cell, tomosyn negatively regulates insulin exocytosis. *Diabetes* 55:574–581, 2006

Exocytosis is delicately regulated via dynamic protein-protein interactions between different protein components localized to the plasma membrane, the secretory vesicle membrane, and the cytoplasm. According to the soluble *N*-ethylmaleimide–sensitive factor attachment protein receptor (SNARE) hypothesis (1,2), the vesicular-SNARE vesicle-associated membrane protein (also called synaptobrevin) interacts with the cognate target-SNAREs syntaxin and synaptosomal-associated protein of 25 kDa (SNAP-25) to form a core complex (also called SNARE complex) (1). The assembly of SNARE proteins between two opposing membranes and the formation of a core complex have been shown to be the key events that initiate membrane fusion and predict the specificity of vesicle fusion (1,2). That the compartmental specificity of cellular membrane fusion is encoded in SNARE proteins is further provided by the observation that these proteins have distinct localization in a cell (3). However, almost any combination of several members of vesicular- and target-SNARE proteins can form a SDS-resistant protein complex (4,5), suggesting that the interactions between SNARE proteins cannot provide all information for vesicle targeting. Additional specificity may be provided by other molecules that interact with SNARE proteins. An example of such a protein is the well-conserved syntaxin-binding protein Sec1/mammalian homolog of the *Caenorhabditis elegans unc-18* gene (Munc-18). There are several Munc-18 isoforms in mammals, which are believed to support different vesicular trafficking events (rev. in 6). Munc-18-1 holds syntaxin in a closed conformation, thereby preventing the binding of SNAP-25 and vesicle-associated membrane protein to syntaxin (7). Moreover, each Munc-18 protein interacts more or less exclusively with one or two syntaxin isoforms, thereby providing further vesicle-targeting specificity (8–13).

The existence of another syntaxin-binding protein, designated tomosyn (tomo = friend in Japanese, syn = syntaxin), has been reported (14). Besides the original tomosyn protein, which has been named m-tomosyn, two further splice variants of tomosyn, designated big (b) and small (s) tomosyn, have been identified (15). The m- and s-tomosyn variants are mainly expressed in the brain, whereas b-tomosyn is found ubiquitously (15). More recently, two distinct genes that drive the expression of seven tomosyn isoforms in the mammalian brain have been described (16). Tomosyn is capable of dissociating Munc-18 from syntaxin 1 and thereby forming a novel complex with syntaxin 1, SNAP-25, and synaptotagmin (14). The COOH-terminal domain of tomosyn spans a SNARE motif that allows tomosyn to form a stable complex with syntaxin 1A and SNAP-25 (17,18). Endogenous expression or overexpression of tomosyn has been shown to cause a reduction of Ca^{2+}-dependent exocytosis (14,19–23). The structural basis for the inhibitory role of tomosyn in exocytosis has recently been presented (24).

In this study, we have investigated isoform expression and cellular localization of tomosyn in insulin-secreting cells as well as the regulatory role of tomosyn in insulin exocytosis. We demonstrate that tomosyn is expressed in the pancreatic β-cell and constitutes an integral part of the exocytotic machinery controlling insulin secretion.

From the [1]Department of Neuroscience, Karolinska Institutet, Stockholm, Sweden; [2]The Rolf Luft Research Center for Diabetes and Endocrinology, Department of Molecular Medicine and Surgery, Karolinska University Hospital, Karolinska Institutet, Stockholm, Sweden; the [3]Department of Pharmacology, University of Aarhus, Aarhus, Denmark; [4]Lilly Research Laboratories, Hamburg, Germany; and the [5]Department of Molecular Biology and Biochemistry, Osaka University Medical School, Suita, Japan.

Address correspondence and reprint requests to Prof. Per-Olof Berggren, The Rolf Luft Research Center for Diabetes and Endocrinology, Department of Molecular Medicine and Surgery, Karolinska University Hospital, L3, Karolinska Institutet, SE-171 76 Stockholm, Sweden. E-mail: per-olof.berggren@ki.se.

Received for publication 5 January 2005 and accepted in revised form 1 December 2005.

J.G. holds stock in Novo Nordisk and Eli Lilly.

GFP, green fluorescent protein; hGH, human growth hormone; Munc-18, mammalian homolog of the *Caenorhabditis elegans unc-18* gene; siRNA, small interfering RNA; SNAP-25, synaptosomal-associated protein of 25 kDa; SNARE, soluble *N*-ethylmaleimide–sensitive factor attachment protein receptor.

RESEARCH DESIGN AND METHODS

Homogenate preparation. Homogenates of cultured cells, β-cell lines, and rat brain from male Sprague-Dawley rats (100–150 g body wt; B & K Universal, Stockholm, Sweden) were prepared as described previously (25).

SDS-PAGE and Western blotting. Five micrograms protein of HIT-T15 cell, RINm5F cell, and rat brain homogenates or 15 μg protein of each HIT-T15 cell fraction was denatured for 20 min at 60°C in SDS-PAGE sample buffer and loaded on a 10% Tris-HCl polyacrylamide SDS-PAGE gel or a 4–15% linear ready gel (Bio-Rad, Hercules, CA). After electrophoresis, protein bands were transferred to polyvinylidene difluoride membranes (Amersham Pharmacia Biotech U.K., Buckinghamshire, U.K.). After blotting, membranes were subsequently incubated overnight with an affinity-purified rabbit polyclonal antiserum to tomosyn (diluted 1:2,000) (14) at 4°C. The blots were washed with buffer containing 50 mmol/l Tris and 150 mmol/l NaCl, pH 7.6, in the presence of 0.5% Tween-20 and incubated for 1 h at room temperature with horseradish peroxidase-conjugated donkey anti-rabbit IgG (diluted 1:5,000; The Jackson ImmunoResearch Laboratories, West Grove, PA). The bands were visualized using the ECL Plus Western blotting analysis system (Amersham International, Amersham, U.K.) and visualized with Hyperfilm (Amersham International).

RT-PCR and DNA sequencing. Brains and pancreatic islets were isolated from male Wistar rats (4 months old; B & K Universal). The rats were killed by cervical dislocation, and the brain and pancreas were quickly removed. Pancreatic islets were isolated by a collagenase digestion technique (26). Total RNA was isolated from RINm5F cells, rat brain, and pancreatic islets using the GenElute Mammalian Total RNA Kit according to the manufacturer's instructions (Sigma). RT-PCR was performed using the SuperScript RT-PCR System (Invitrogen, Gaithersburg, MD). Specific primers for b-, m-, and s-tomosyn (15) were synthesized (Proligo France, Paris, France), corresponding to nucleotides 2138–2159 (5′-CTCCGACTTCCGGTTCTTCCTC-3′) and 2492–2473 (5′-TTCAGCGTGATGACAAAGGC-3′) of b-tomosyn (GenBank accession number AF118889), 2488–2509 (5′-CTCCGACTTCCGCAAAGATGTC-3′) and 2734–2715 (5′-TTCAGCGTGATGACAAAGGC-3′) of m-tomosyn (GenBank accession number RRU92072), and 2138–2158 (5′-CTCCGACTTC CGATGTGAAAG-3′) and 2333–2314 (5′-TTCAGCGTGATGACAAAGGC-3′) of s-tomosyn (GenBank accession number AF118890), resulting in PCR products of 350, 230, and 200 bp, respectively. The RT-PCRs were performed using 10 pmol of each primer and the following program: 30 min at 50°C and 2 min at 94°C, followed by 40 cycles at 94°C for 1 min, annealing at 50°C (m- and s-tomosyn) or 60°C (b-tomosyn) for 1 min and extension at 72°C for 1 min, ending with a final extension at 72°C for 7 min. The amplified PCR products were separated by electrophoresis on a 2% agarose gel and visualized by ethidium bromide staining. A 1-kb DNA ladder (Invitrogen) was used as size marker. After ethanol precipitation, the PCR-amplified DNA fragments were directly sequenced by an ABI Prism 377 sequencer (Applied Biosystems, Foster City, CA) using appropriate primers and a BigDye Terminator v3.1 Cycle Sequencing kit (Applied Biosystems).

Subcellular fractionation. Mouse pancreatic islets were isolated from 10- to 12-month-old *ob/ob* mice as previously described (26,27). *Ob/ob* islets are composed of >90% β-cells (27,28). Isolated islets from *ob/ob* mice were incubated in a humidified atmosphere with 5% CO_2 for 1 h in RPMI-1640 culture medium containing 3 mmol/l glucose supplemented with 10% (v/v) heat-inactivated FCS, 100 IU/ml penicillin, 100 μg/ml streptomycin, and 2 mmol/l L-glutamine. The islets were washed, homogenized, and centrifuged as previously described (29). Fifteen to 16 fractions (300 μl each) were collected from the top of the gradient. The linearity of the gradients was examined by measuring the refractive index of each fraction. Equal amounts of protein from each fraction were separated on 10% Bis-Tris NU-PAGE gels (Invitrogen) and transferred to polyvinylidene difluoride membranes (Amersham Biosciences). Membranes were blocked in PBS containing 5% milk powder and 0.025% Tween-20 (VWR International) for 1 h and then probed with primary antibodies overnight at 4°C (tomosyn 1:5,000; syntaxin 1 1:4,000 [mouse monoclonal anti–syntaxin 1 antibody, clone HPC-1; Sigma]; and insulin 1:5,000 [rabbit polyclonal anti-insulin antibody, H-86; Santa Cruz Biotechnology]). After washing, membranes were incubated with horseradish peroxidase-conjugated immunoglobulins for 90 min at room temperature. Immunoreactive bands were detected by enhanced chemiluminescence (ECL Plus; Amersham Biosciences), after exposure to hyperfilm (Amersham Biosciences) or by using a CCD camera (LAS 1000; Fuji Photo Film) that provides optimal linearity of signal intensity.

Immunoprecipitation. Protein A-Sepharose CL-4B (Amersham Biosciences, Uppsala, Sweden) was rinsed three times with lysis buffer (20 mmol/l Tris pH 7.5, 150 mmol/l NaCl, 1 mmol/l EGTA, 1% NP-40, and protease inhibitor cocktail; Roche, Basel, Switzerland). Lysate of HIT-T15 cells and lysis buffer were precleared at 4°C for 2 h with protein A-Sepharose. The beads were spun down for 2 min at 7,000*g*. The supernatants were incubated at 4°C overnight on a rotatory shaker with affinity-purified rabbit antiserum to tomosyn (14) or nonimmune rabbit IgG as control, followed by incubation with protein A-Sepharose at 4°C for 2 h. The beads were collected by centrifugation and washed three times at 4°C with lysis buffer. The beads were further washed twice with lysis buffer without Triton X-100. After the final wash, the beads were resuspended in 8 μl 5× SDS-PAGE sample buffer, heated for 20 min in a water bath at 60°C, and centrifuged. The supernatants were resolved by electrophoresis on 18% polyacrylamide SDS-PAGE gel and blotted using the monoclonal antibody against syntaxin 1 (diluted 1:2,000).

Immunofluorescence histochemistry. Male Sprague-Dawley rats (80–100 g body wt; B & K Universal) were anesthetized with sodium pentobarbital (Mebumal; 40 mg/kg i.p.) and perfused via the ascending aorta with Ca^{2+}-free Tyrode's solution (37°C), followed by an ice-cold mixture of formalin-picric acid (4% paraformaldehyde and 0.4% picric acid in 0.16 mol/l phosphate buffer, pH 6.9). Sections were cut at 14 μm thickness in a cryostat (Dittes, Heidelberg, Germany) and processed for immunofluorescence histochemistry as described previously (21). Briefly, monolayers of HIT-T15 cells or pancreatic β-cells both fixed by immersion or sections were incubated with rabbit antiserum to tomosyn (diluted 1:400) (14) overnight at 4°C or combined with mouse monoclonal antibodies to insulin (diluted 1:600,000; clone K36aC10; catalog no. I-2018; Sigma), glucagon (diluted 1: 6,000; catalog no. G-2654; Sigma), somatostatin (diluted 1:600) (30), or guinea-pig antiserum to pancreatic polypeptide (diluted 1:12,000; lot no. RPP-63; Linco Research, St. Charles, MO). The combinations were visualized using a mixture of Cy5-conjugated donkey anti-rabbit (diluted 1:250) and fluorescein isothiocyanate-conjugated donkey anti-mouse (diluted 1:80) or guinea-pig (diluted 1:80) secondary antibodies (all from Jackson ImmunoResearch) or Alexa Fluor 546 goat anti-rabbit IgG (diluted 1:80; Molecular Probes, Leiden, The Netherlands). Specimens were examined in a Bio-Rad RadiancePlus or a Leica confocal laser scanning system.

Cell culture. HIT-T15 and RINm5F cells were grown to 70% confluency in 175 cm^2 Nunc flasks (Nunc, Naperville, IL) using RPMI-1640 (Invitrogen) supplemented with FCS (10%, v/v), glutamine (2 mmol/l), streptomycin (100 μg/ml), penicillin (100 IU/ml), and glucose (11 mmol/l). The cells were cultured at 37°C in a humidified incubator with 95% air/5% CO_2. Pancreatic β-cells were isolated from *ob/ob* mice or NMRI mice (18–25 g; Bomholtgård, Ry, Denmark). The mice were killed by cervical dislocation, and the pancreas was quickly removed. The pancreatic islets were isolated by collagenase (3 mg/ml; type XI from Sigma) digestion, and the islets were dispersed into single cells by shaking in a Ca^{2+}-free solution. The resulting cell suspension was plated on glass coverslips in Nunc Petri dishes and maintained for up to 4 days in RPMI-1640 tissue-culture medium (Invitrogen) supplemented with 10% (v/v) heat-inactivated FCS, 100 IU/ml penicillin, and 100 mg/ml streptomycin. INS-1E cells were cultured in a humidified atmosphere containing 5% CO_2 in complete medium composed of RPMI-1640 supplemented with 5% heat-inactivated FCS, 1 mmol/l sodium pyruvate, 50 μmol/l 2-mercaptoethanol, 2 mmol/l glutamine, 10 mmol/l HEPES, 100 units/ml penicillin, and 100 μg/ml streptomycin as described previously (31). The maintenance culture was passaged once a week by gentle trypsinization, and cells were seeded at a density of 4×10^4 cells/cm^2, i.e., 3×10^6 cells, in 75-cm^2 Falcon bottles (Nunc) with 20 ml complete medium.

Cell transfection. Single mouse pancreatic β-cells, HIT-T15 cells, or INS-1E cells were transfected with pIRES2-EGFP (representing mock-transfected cells for electrophysiology), a combination of pIRES2-EGFP and pEF-BOS-control (representing mock-transfected cells for immunohistochemistry), or a combination of pIRES2-EGFP and pEF-BOS-tomosyn (14) alternatively with control small interfering RNA (siRNA) or tomosyn siRNA in the expression vector pSIREN-RetroQ (BD Biosciences Clontech, San José, CA) using the Lipofectamine 2000 technique (Invitrogen). Two days after transfection, cells expressing enhanced green fluorescent protein (GFP) were selected for capacitance measurements or rinsed in cold phosphate-buffered saline and fixed by immersion in 4% formaldehyde in phosphate buffer.

Electrophysiology. Exocytosis was monitored in single β-cells as changes in cell capacitance using an EPC-9 patch-clamp amplifier Pulse software (HEKA Elektronik, Lambrecht/Pfalz, Germany), as described previously (32). In Fig. 4, exocytosis was elicited by trains of ten 500-ms voltage-clamp depolarizations and went from −70 to 0 mV using the perforated patch whole-cell configuration. The pipette solution consisted of (mmol/l): 76 Cs_2SO_4, 10 NaCl, 10 KCl, 1 $MgCl_2$, and 5 HEPES (pH 7.35 with CsOH). Electrical contact with the cell interior was established by adding 0.24 mg/ml amphotericin B to the pipette solution. Perforation required a few minutes, and the voltage clamp was considered satisfactory when the series conductance (G_{series}) was constant and >35–40 nS. In Fig. 6, exocytosis was elicited by infusion of Ca^{2+} containing pipette solution to the cell interior. The interval between two successive points was 0.2 s, and the measurements of cell capacitance were initiated <5 s after establishment of the standard whole-cell configuration. In

these experiments, the extracellular solution was composed of (in mmol/l) 138 NaCl, 5.6 KCl, 2.6 $CaCl_2$, 1.2 $MgCl_2$, 5 HEPES (pH 7.4 with NaOH), and 5 D-glucose. The pipette solution consisted of (in mmol/l) 125 potassium glutamate, 10 KCl, 10 NaCl, 1 $MgCl_2$, 5 HEPES, 3 Mg-ATP, 10 EGTA, and 0, 2, 5, 7, 9, and 9.5 $CaCl_2$ (pH 7.15 with KOH). The free Ca^{2+} concentration of the resulting buffers ranged from 0.03 to 10 μmol/l using the binding constants of Martell and Smith (33,34). During the experiments, the cells were situated in an experimental chamber with a volume of 0.4 ml, which was continuously superfused at a rate of 1.5–2 ml/min to maintain the temperature at ~33°C. Forskolin was dissolved in dimethylsulfoxide (final concentration: 0.01–0.1%). All other chemicals were from Sigma.

Human growth hormone transfection and secretion. For transient transfection experiments, INS-1E cells (6×10^5 cells) were cotransfected with 2 μg pCMV-hGH and 2 μg plasmid of interest using Lipofectamine 2000 (Invitrogen), according to the manufacturer's specification. Immediately after transfection, cells were seeded in 48-multiwell plates (2×10^5 cells per well) and cultured for 48 h. Incubation and secretion experiments were performed as described previously (25). Human growth hormone (hGH) levels in the various samples were measured using an enzyme-linked immunosorbent assay (Roche) according to the manufacturer's instructions.

cAMP determinations. Tomosyn- or mock-transfected INS-1E were seeded in 48-multiwell plates (4,000 cells/well). After 48 h of culture, cells were washed once and preincubated at 37°C in Krebs-Ringer bicarbonate HEPES buffer containing 1 mmol/l glucose and 0.5 mmol/l isobutylmethylxanthine and 2 mg/ml BSA for 1 h and incubated for another 15 min in the same buffer with or without 5 μmol/l forskolin. The reaction was stopped by addition of 50 mmol/l HCl and neutralized with NaOH. Concentration of cAMP was determined by a cAMP ^{125}I-scintillation proximity assay (Amersham).

Data analysis. Results are presented as means ± SE for the indicated number of experiments. Statistical significance was evaluated using Student's *t* test or Dunnett's test.

RESULTS

Tomosyn protein is present in insulin-secreting cells. To examine tomosyn expression, brain tissue and the β-cell lines RINm5F and HIT-T15 were homogenized and separated by SDS-PAGE followed by immunoblotting. Both in the different cell lines and in rat brain homogenates, an affinity-purified rabbit polyclonal antiserum raised against tomosyn detected a strong band of ~130 kDa (Fig. 1*A*).

Tomosyn b-, m-, and s-mRNA variants are present in insulin-secreting cells. To examine the expression of tomosyn isoform mRNA in rat pancreatic islets and insulin-secreting RINm5F cells, we performed RT-PCR using b-, m-, and s-tomosyn–specific primers. Amplified PCR products with the expected size of 350, 230, and 200 bp were detected in RINm5F cell, rat islet, and brain RNA, representing b-, m-, and s-tomosyn, respectively (Fig. 1*B*). The identity of the products was confirmed by DNA sequencing.

Tomosyn in subcellular fractions of insulin-secreting cells. The subcellular localization of tomosyn immunoreactivity in insulin-secreting β-cells was examined using subcellular fractions of islets obtained from *ob/ob* mice. Tomosyn was mainly demonstrated in fractions 2–4 (Fig. 1*C*). Weaker tomosyn immunoreactivity was also seen in fractions 5–15 (Fig. 1*C*). Syntaxin 1 was primarily observed in fractions 4–11, whereas insulin was present in fractions 8–15 (Fig. 1*C*). Tomosyn thus cofractionates with syntaxin 1 rather than insulin. Fractions 2–4 represent soluble proteins, fractions 5–11 represent membrane fractions, and fractions 12–14 represent heavier organelles.

Tomosyn coprecipitates with syntaxin 1 in insulin-secreting cells. To evaluate the possible association of tomosyn with syntaxin 1, immunoprecipitation was performed in HIT-T15 cell homogenates using an affinity-purified polyclonal antiserum against tomosyn or nonimmune rabbit IgG as a control. Proteins bound to the beads were subjected to SDS-PAGE followed by immunoblotting using an anti-syntaxin antibody. The presence of a 35-kDa band corresponding to syntaxin 1 was demonstrated in extracts of HIT-T15 cells, immunoprecipitated with tomosyn antiserum (Fig. 1*D*, *lane 2*). No syntaxin immunoreactivity was observed in HIT-T15 cell homogenate or lysis buffer after incubation with nonimmune rabbit IgG (Fig. 1*D*; *lanes 3* and *4*, respectively; *lane 1*, normal HIT-T15 cell homogenate).

Tomosyn immunoreactivity in pancreatic endocrine cells. To examine the cellular distribution of tomosyn, we performed immunohistochemistry on islets of Langerhans from rat. Tomosyn immunoreactivity was detected in virtually all islets cells (Fig. 2). Double-labeling immunofluorescence histochemistry of rat pancreatic islets demonstrated tomosyn immunoreactivity in insulin- (Fig. 2*A–C*), glucagon- (Fig. 2*D–F*), pancreatic polypeptide– (Fig. 2*G–I*), and somatostatin- (Fig. 2*J–L*) containing cells. In addition, tomosyn immunoreactivity was demonstrated in nerve fibers and terminals present around blood vessels and extending into the islets. Weaker tomosyn immunoreactivity was also seen in exocrine cells of the rat pancreas (data not shown).

Tomosyn inhibits Ca^{2+}-evoked exocytosis in mouse β-cells. We investigated the effect of m-tomosyn overexpression on the exocytotic response in pancreatic β-cells. For this purpose, we cotransfected β-cells with tomosyn and EGFP plasmids. Figure 3 shows mouse β-cells and HIT-T15 cells overexpressing tomosyn (see Fig. 3*D–F* and *M–O*, respectively) or with downregulated tomosyn expression induced by tomosyn siRNA (see Fig. 3*G–I* and *P–R*, respectively).

In Fig. 4*A*, a train of 10 500-ms voltage-clamp depolarizations was applied to evoke exocytosis in single mock-transfected mouse β-cells and in tomosyn-overexpressing cells. The exocytotic response was measured as an increase in membrane capacitance. On average, the increase in membrane capacitance under control conditions (mock transfection) was 22 ± 7 and 63 ± 12 fF ($n = 7$) evoked by the first depolarization and the total train, respectively (Fig. 4*C* and *D*). The integrated Ca^{2+} current measured at the end of the train, when secretion had ceased, was only reduced by 17 ± 9% ($n = 7$) with respect to the first depolarization (data not shown). However, in tomosyn-overexpressing β-cells, the exocytotic response was significantly diminished. The increase in membrane capacitance was 8 ± 3 fF ($P < 0.05$; $n = 6$) during the first depolarization, and the total increase was 27 ± 9 fF ($P < 0.05$; $n = 6$) during the train (Fig. 4*C* and *D*). No difference in the peak or integrated Ca^{2+} current was observed between mock- and tomosyn-transfected cells (data not shown). We repeated the same protocol in the presence of 10 μmol/l forskolin (Fig. 4*B*). In mock-transfected cells, the exocytotic response was strongly enhanced, the increase in membrane capacitance during the first depolarization was 81 ± 10 fF ($n = 7$), and the total increase amounted to 283 ± 22 fF ($n = 7$) (Fig. 4*C* and *D*). Again, overexpression of tomosyn strongly decreased exocytosis, and the increase in membrane capacitance was 13 ± 5 fF ($P < 0.05$; $n = 6$) and 69 ± 13 fF ($P < 0.05$; $n = 6$) during the first depolarization and total train, respectively (Fig. 4*C* and *D*). Importantly, the reduction in the exocytotic response in cells overexpressing tomosyn does not result from a reduction in cellular cAMP content (Table 1). These data suggest that tomosyn exerts a strong inhibitory action

on Ca^{2+}-evoked exocytosis in pancreatic β-cells. Interestingly, downregulation of endogenous levels of tomosyn in mouse β-cells using siRNA directed against all three isoforms (Fig. 3) was associated with stimulation of exocytosis in response to a train of membrane depolarizations compared with cells transfected with control siRNA (Fig. 4*E*). A similar enhancement of exocytosis was observed in forskolin-stimulated cells after siRNA downregulation of tomosyn. The histograms in Fig. 4*F* and *G* show that downregulation of tomosyn was associated with stimulation of exocytosis evoked by both the first membrane depolarization and the entire train.

Tomosyn inhibits glucose- and forskolin-induced human growth hormone secretion in insulin-secreting cells. To confirm that the effect of overexpression of tomosyn on insulin secretion as observed by capacitance measurements was due to inhibition of exocytosis and not increased endocytosis, a secretion assay using hGH was applied on the insulinoma cell line INS-1E. In control cells or in cells cotransfected with pCMV5-hGH and empty vector (pcDNA3; mock), there was a significant stimulation of hGH release ($P < 0.05$) after addition of 16.7 mmol/l glucose compared with 3 mmol/l glucose (Fig. 5*A*). Cotransfection with pCMV5-hGH and tomosyn plasmid revealed a significantly reduced release of hGH ($P < 0.05$) compared with cells cotransfected with pCMV5-hGH and empty vector (pcDNA3; mock) in the presence of 16.7 mmol/l glucose (Fig. 5*A*). Addition of forskolin to cells cotransfected in parallel with pCMV5-hGH and empty vector (pcDNA3; mock), showed a significant stimulation after addition of 16.7 mmol/l glucose compared with mock-transfected cells not treated with forskolin ($P < 0.05$) (Fig. 5*A*). When cells were cotransfected with pCMV5-hGH and tomosyn plasmid, a significant reduction ($P < 0.01$) was seen after addition of forskolin compared with mock-transfected (empty vector) cells in the presence of 16.7 mmol/l glucose (Fig. 5*A*).

Figure 5*B* shows that siRNA downregulation of tomosyn was associated with stimulation of hGH release in high glucose–containing but not low glucose–containing medium. The stimulation of hGH secretion was also observed in the presence of forskolin (Fig. 5*B*).

Tomosyn decreases Ca^{2+} sensitivity in exocytosis. To examine whether tomosyn overexpression decreased insulin secretion by changing the Ca^{2+} dependency, exocytosis was elicited by intracellular infusion with Ca^{2+}-EGTA buffers with free Ca^{2+} concentrations in the range of 0.03 to 10 μmol/l. The cell capacitance was significantly reduced ($P < 0.05$ and $P < 0.01$) in mouse β-cells expressing tomosyn-transfected cells compared with mock-transfected cells (Fig. 6). These data suggest that in cells overexpressing tomosyn, exocytosis is triggered at higher Ca^{2+} concentrations.

TABLE 1
Effects of tomosyn and forskolin on cAMP production in INS-1E cells

Condition	cAMP production (fmol/1000 cells)	*n*
Mock	11.3 ± 2.7	5
Tomosyn	12.0 ± 3.3	5
Forskolin	41.2 ± 2.1*	5
Forskolin + tomosyn	40.2 ± 4.1	5

Data are means ± SE. *$P < 0.01$ vs. mock transfected.

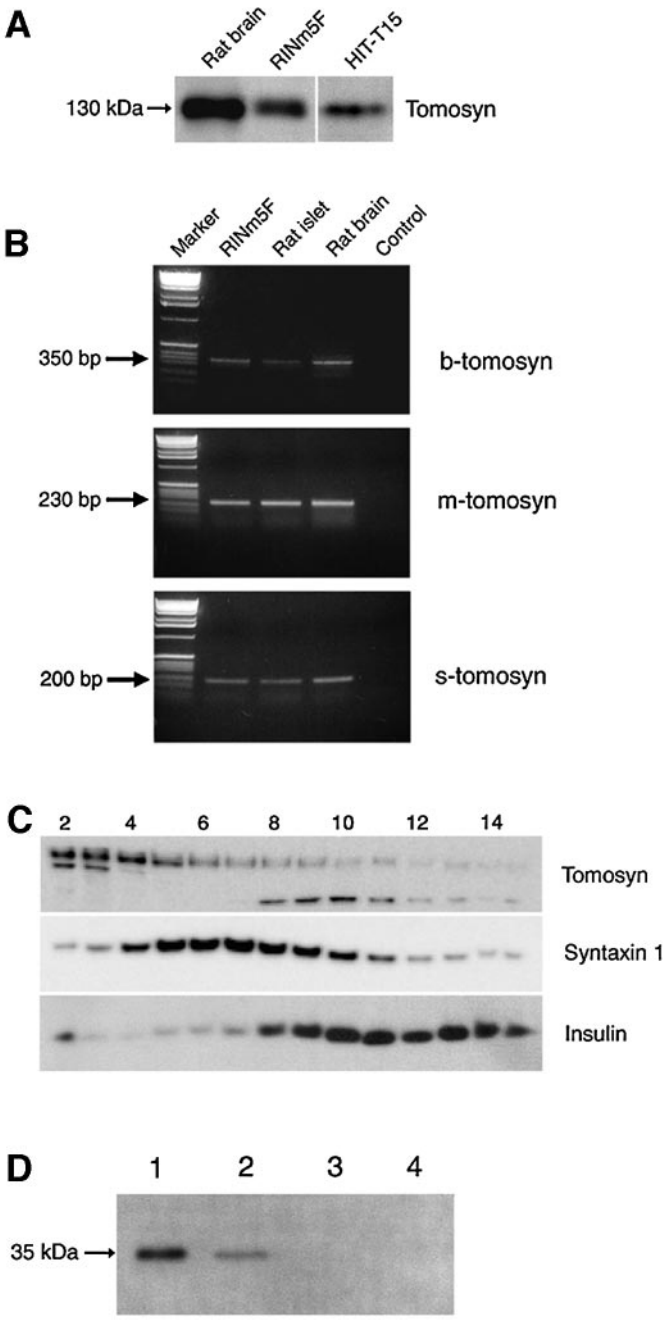

FIG. 1. Tomosyn protein and mRNA are present and associate with syntaxin 1 in β-cells. *A*: Detection by immunoblotting of a 130-kDa protein corresponding to the expected size of tomosyn in rat brain and in insulin-secreting RINm5F and HIT-T15 cells. *B*: RT-PCR with tomosyn isoform–specific primers shows expression of PCR products corresponding to b-, m-, and s-tomosyn mRNAs in insulin-secreting RINm5F cells, rat pancreatic islets, and brain. Control, absence of RNA. Marker = 1-kb DNA ladder. *C*: Subcellular localization of tomosyn immunoreactivity in insulin-secreting β-cells from islets obtained from *ob/ob* mice. Tomosyn is mainly present in fractions 2–4. Weaker tomosyn immunoreactivity is also seen in fractions 5–15. Syntaxin is primarily observed in fractions 4–11, whereas insulin is present in fractions 8–15. Fractions 2–4 represent soluble proteins, fractions 5–11 represent membrane protein, and fractions 12–14 represent heavier organelles. Tomosyn cofractionates with syntaxin 1 rather than insulin. This experiment was repeated three times with similar results. *D*: HIT-T15 cell homogenate subjected to immunoprecipitation using an antiserum to tomosyn. Normal rabbit IgG was used as a control. The immunoprecipitates were subjected to SDS-PAGE followed by Western blotting using an anti–syntaxin 1 antibody. *Lane 1*, normal HIT-T15 cell homogenate; *lane 2*, immunoprecipitate with the antiserum to tomosyn; *lane 3*, immunoprecipitate with nonimmune rabbit IgG; *lane 4*, lysis buffer that has been incubated with normal rabbit IgG.

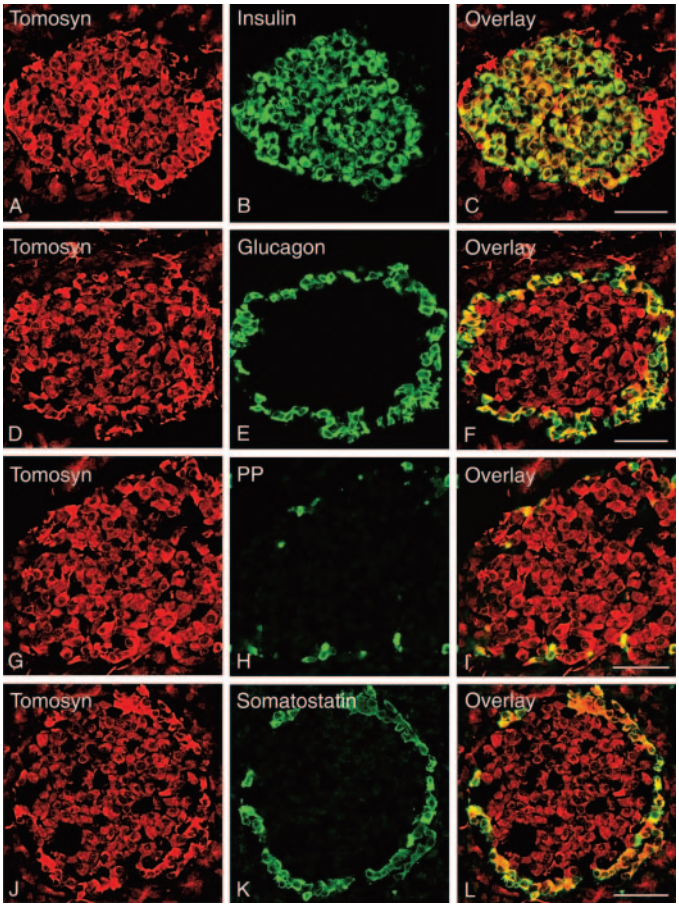

FIG. 2. Localization of tomosyn in pancreatic endocrine cells. Tomosyn immunoreactivity (*A*, *D*, *G*, and *J*; red color) is present in insulin-containing (*B*), glucagon-containing (*E*), pancreatic polypeptide–containing (PP) (*H*), or somatostatin-containing (*K*) islet cells (green color). Colocalization of tomosyn immunoreactivity with insulin, glucagon, pancreatic polypeptide, and somatostatin, respectively, is indicated by yellow color in overlay images (*C*, *F*, *I*, and *L*). Bars = 50 μm.

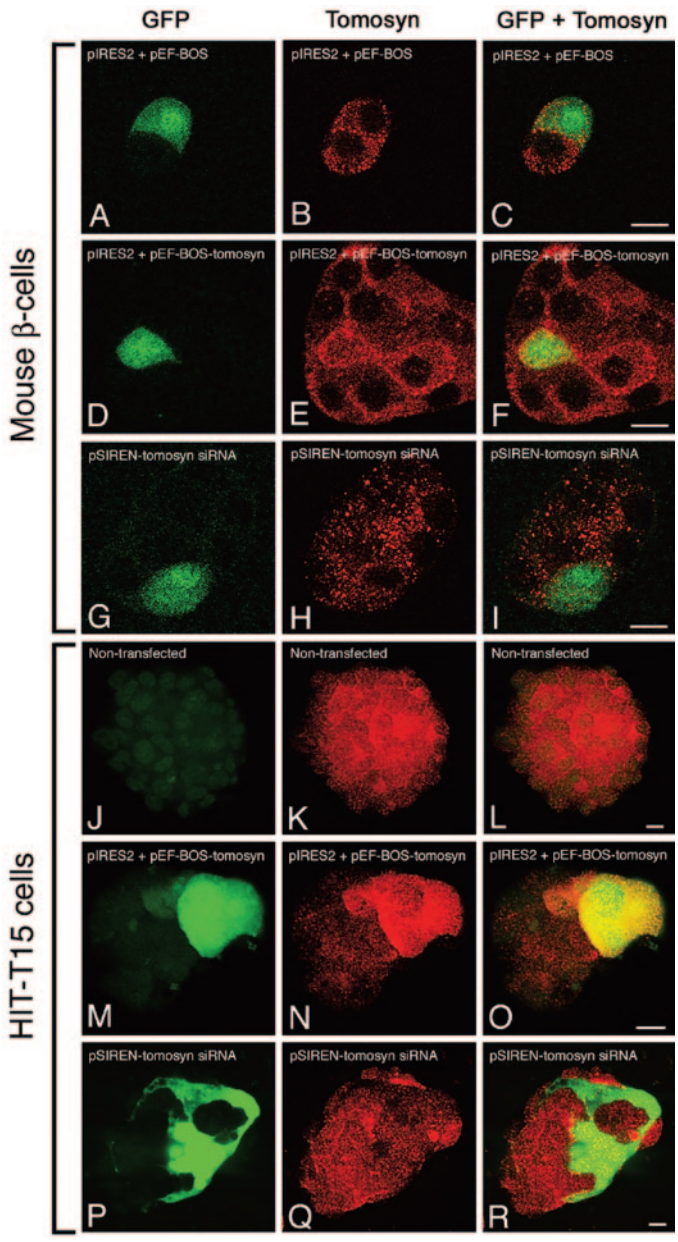

FIG. 3. Transfection of insulin-producing cells. Images of cultured insulin-producing mouse β-cells (*top panels*; *A–I*) or HIT-T15 cells (*bottom panels*; *L–R*) either mock-transfected (pIRES2-EGFP + pEF-BOS) (*A–C*), transfected with pIRES2-EGFP + pEF-BOS-tomosyn (tomosyn overexpression; *D–F* and *M–O*), or tomosyn siRNA in the expression vector pSIREN-RetroQ expressing GFP (*G–I* and *P–R*). GFP (*left panels*; *A*, *D*, *G*, *J*, *M*, and *P*) is illustrated in green, and tomosyn immunoreactivity (*middle panels*; *B*, *E*, *H*, *K*, *N*, and *Q*) is shown in red. Colocalization (overlay) of GFP-induced fluorescence and tomosyn immunoreactivity is shown in yellow (*right panels*; *C*, *F*, *I*, *L*, *O*, and *R*). Note presence of strong tomosyn immunoreactivity in tomosyn overexpressing cells (*D–F* and *M–O*) and weaker tomosyn immunoreactivity in cells transfected with tomosyn siRNA (*G–I* and *P–R*). Bars = 10 μm.

DISCUSSION

The present results show that three tomosyn isoforms are expressed in insulin-secreting β-cells and that tomosyn is negatively involved in the regulation of Ca^{2+}-dependent insulin exocytosis. In agreement with previous reports (14,20,35), we demonstrate that tomosyn coprecipitates with syntaxin 1, supporting an intimate association between tomosyn and syntaxin also in β-cells. Previous studies have shown that m- and s-tomosyn are mainly expressed in the brain, whereas b-tomosyn is found ubiquitously (15). Against this background, it is noteworthy that all three isoforms were expressed in endocrine β-cells.

In mock-transfected cells, we observed that depolarization elicited a massive exocytotic response and that membrane capacitance ceased to increase during a train of depolarizations. Exhaustion of the exocytotic capacity during the train is likely to reflect depletion of a readily releasable pool of granules rather than inactivation of the Ca^{2+} current with resultant suppression of Ca^{2+}-induced exocytosis. This is suggested by the observation that the integrated Ca^{2+} current measured at the end of the train, when secretion had ceased, was only reduced by 17 ± 9% with respect to the first depolarization. In tomosyn-overexpressing β-cells, we found that evoked exocytotic response was dramatically decreased. In the meantime, no difference in the peak or integrated Ca^{2+} current was observed between mock- and tomosyn-transfected cells. We thus exclude the possibility that the inhibition of the exocytotic response in tomosyn-overexpressing β-cells resulted from a reduction in Ca^{2+} influx. The same experiment was repeated in the presence of forskolin. It was found that the exocytotic response was enhanced in mock-transfected cells, whereas overexpression of tomosyn decreased exocytosis. These data suggest that tomosyn exerts a pronounced inhibitory action on Ca^{2+}- and

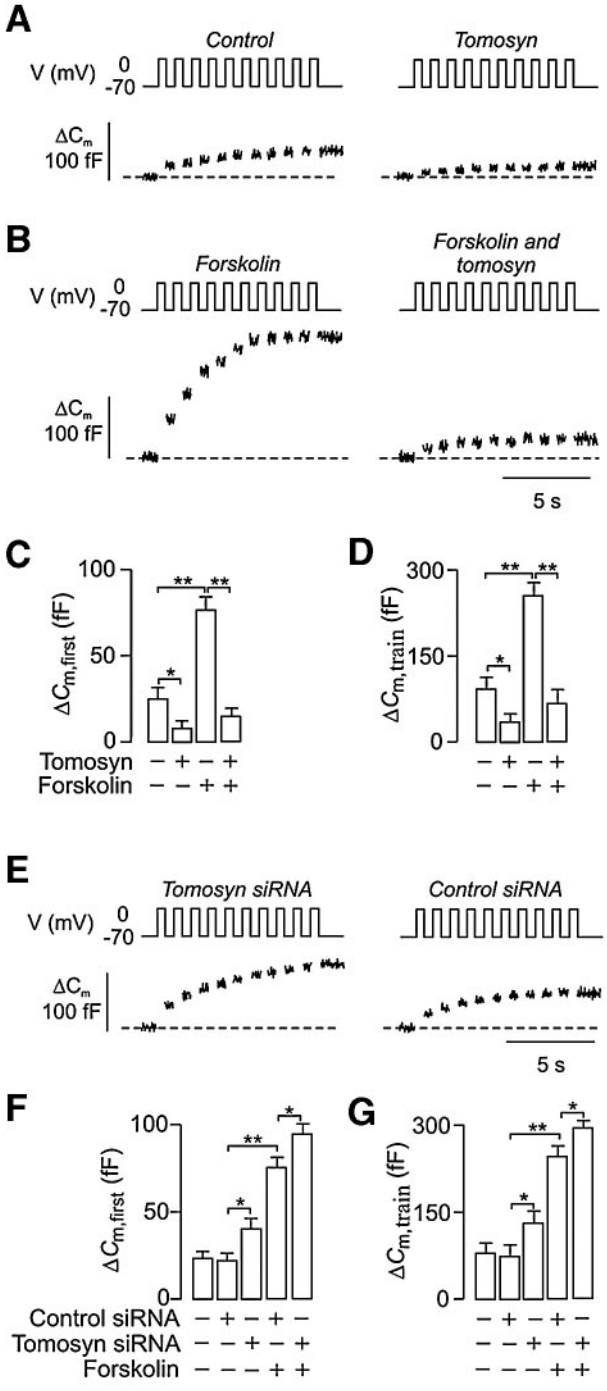

FIG. 4. Tomosyn negatively regulates Ca^{2+}-evoked exocytosis in mouse β-cells. *A*: Increase in membrane capacitance reflecting exocytosis of insulin-containing secretory granules from single mouse β-cells. Exocytosis was evoked by a train of 10 500-ms depolarizations from −70 to 0 mV applied at 1 Hz and performed under control conditions (mock transfection) and in cells overexpressing tomosyn. *B*: Similar to *A*, but the experiments were conducted in the presence of 10 μmol/l forskolin. *C* and *D*: Histograms summarizing the increases in cell capacitance during the first membrane depolarization ($\Delta C_{m,first}$; *C*) and in response to the whole train ($\Delta C_{m,train}$; *D*) in mock-transfected cells (−) and in cells overexpressing tomosyn (+) and in the absence and presence of 10 μmol/l forskolin in the extracellular solution. *E*: Similar to *A*, except that cells were transfected with tomosyn siRNA (*left*) or control siRNA (*right*). Histograms summarizing the increases in cell capacitance during the first membrane depolarization ($\Delta C_{m,first}$; *F*) and in response to the whole train ($\Delta C_{m,train}$; *G*) in tomosyn or control siRNA-transfected cells in the absence and presence of 10 μmol/l forskolin in the extracellular solution. Data are means ± SE of six to seven experiments. *$P < 0.5$; **$P < 0.01$.

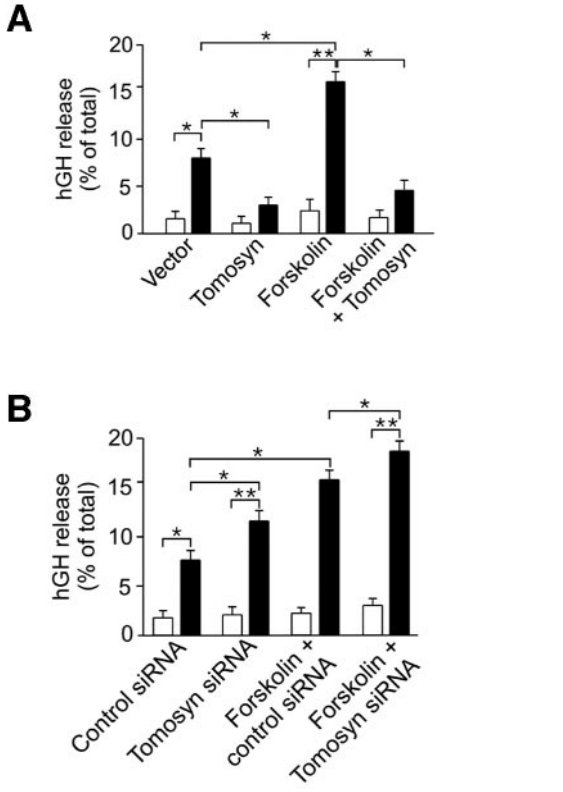

FIG. 5. Tomosyn negatively regulates secretion in insulin-secreting cells. *A*: Overexpression of tomosyn inhibits glucose- and forskolin-induced hGH secretion in INS-1E cells. Cells were cotransfected in parallel either with pCMV5-hGH and empty vector (pcDNA3; mock) or with pCMV5-hGH and tomosyn plasmid. hGH secretion was measured in Krebs-Ringer bicarbonate HEPES buffer with either 3 (□) or 16.7 (■) mmol/l glucose. hGH release is depicted as secreted hGH in percentage of total hGH. *B*: Similar to *A*, except that cells were transfected with tomosyn siRNA or control siRNA. The experiments were conducted in the absence and presence of 10 μmol/l forskolin in the extracellular solution. Data are means ± SE of three different experiments (each in triplicate). *$P < 0.05$; **$P < 0.01$.

cAMP-evoked exocytosis in pancreatic β-cells. The inhibitory role of tomosyn in insulin exocytosis was further supported by inhibition of tomosyn expression using siRNA, which was associated with an increase in exocytosis and hGH release.

Hatsuzawa et al. (17) reported that overexpression of tomosyn in PC12 cells resulted in a massive reduction of exocytosis but that the kinetics/release parameters of individual exocytotic events remained unchanged (17). It was therefore suggested that tomosyn overexpression strongly diminishes the number of rapidly releasing granules and that tomosyn governs the readiness of the secretory organelles for exocytosis rather than the molecular mechanism of membrane fusion (17). Further support for this hypothesis has been presented by Yizhar et al. (21), showing that tomosyn overexpression causes a 50% reduction in the number of fusion-competent vesicles. Because the number of docked vesicles and the fusion kinetics of single vesicles were not altered, it was suggested that tomosyn inhibits the priming step (21). Experiments further supported that the reduction in secretion is caused by a shift in the Ca^{2+} dependence of release, suggesting that secretion is not entirely blocked by tomosyn but occurs at higher Ca^{2+} concentrations and that tomosyn impairs the efficacy of vesicle pool refilling (19). Our finding that overexpression of tomosyn decreased Ca^{2+} sensitivity in

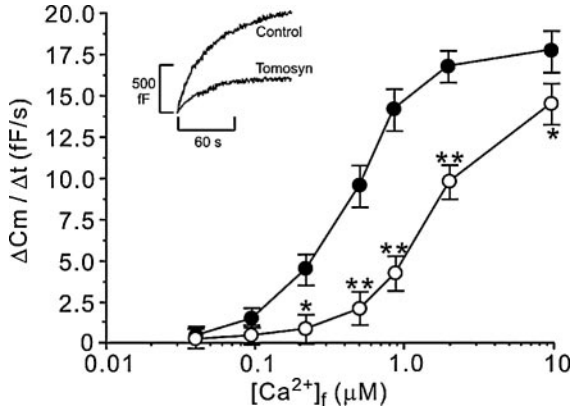

FIG. 6. Tomosyn decreases Ca^{2+} sensitivity in exocytosis. Exocytosis was elicited by intracellular infusion with Ca^{2+}-EGTA buffers with free Ca^{2+} concentrations of 0.03–10 μmol/l in either mock-transfected cells (●) or in mouse β-cells overexpressing tomosyn (○). Changes in cell capacitance were measured 2 days after transfection and are depicted as mean rates of increase in cell capacitance ($\Delta C_m/\Delta t$) during the first 60 s after establishment of the whole-cell configuration. The *inset* shows increases in cell capacitance observed during the first 2 min after establishment of the standard whole-cell configuration elicited by intracellular infusion in mock-transfected (control) and tomosyn-transfected cells using a pipette solution with a free Ca^{2+} concentration of 0.87 μmol/l. Throughout the recordings, the cells were clamped at −70 mV to avoid activation of the voltage-dependent Ca^{2+}-channels that would otherwise interfere with the capacitance measurements. *$P < 0.05$ and **$P < 0.01$ vs. mock-transfected cells.

mouse β-cell exocytosis is thus supportive of the model proposed by Yizhar et al. (21).

The inhibitory effect of tomosyn on exocytosis has been assumed to result from the interaction with syntaxin and formation of nonfunctional SNARE complexes. However, recent observations show that tomosyn can negatively regulate exocytosis independent of syntaxin. Mutations that disrupt the binding of tomosyn to syntaxin 1 in PC12 cells do not reduce the inhibitory effect of tomosyn on exocytosis (20). These findings imply that an alternative protein-protein interaction may be involved. More recently, it has been shown that tomosyn is a target for cAMP-dependent protein kinase (36). In neurons, cAMP-dependent protein kinase–catalyzed phosphorylation of tomosyn acts as an off switch for tomosyn by blocking its inhibitory function on the formation of the SNARE complex and thereby upregulating the size of the readily releasable pool of synaptic vesicles (36).

In conclusion, tomosyn is expressed by pancreatic β-cells and negatively regulates insulin secretion. Further studies may reveal the precise role(s) of tomosyn in the regulation of exocytosis and in type 2 diabetes, a disease characterized by an impaired stimulus-secretion coupling.

ACKNOWLEDGMENTS

This work was supported by the grants from the Swedish Research Council, The Swedish Diabetes Association, The Novo Nordisk Foundation, The Danish Diabetes Association, The Berth von Kantzows Foundation, The Family Stefan Persson Foundation, and The Edla and Erik Smedbergs Foundation and by funds from Karolinska Institutet and University of Aarhus.

We thank Dr. Q. Zhang, N. Dekki, and R. Nilsson for their help. We thank H. Rotter for help and technical assistance.

REFERENCES

1. Söllner T, Whiteheart SW, Brunner M, Erdjument-Bromage H, Geromanos S, Tempst P, Rothman JE: SNAP receptors implicated in vesicle targeting and fusion. *Nature* 362:318–324, 1993
2. Rothman JE: Mechanisms of intracellular protein transport. *Nature* 372: 55–63, 1994
3. McNew JA, Parlati F, Fukuda R, Johnston RJ, Paz K, Paumet F, Söllner TH, Rothman JE: Compartmental specificity of cellular membrane fusion encoded in SNARE proteins. *Nature* 407:153–159, 2000
4. Fasshauer D, Antonin W, Margittai M, Pabst S, Jahn R: Mixed and non-cognate SNARE complexes: characterization of assembly and biophysical properties. *J Biol Chem* 274:15440–15446, 1999
5. Yang B, Gonzalez L Jr, Prekeris R, Steegmaier M, Advani RJ, Scheller RH: SNARE interactions are not selective: implications for membrane fusion specificity. *J Biol Chem* 274:5649–5653, 1999
6. Toonen RF, Verhage M: Vesicle trafficking: pleasure and pain from SM genes. *Trends Cell Biol* 13:177–186, 2003
7. Yang B, Steegmaier M, Gonzalez LC Jr, Scheller RH: nSec1 binds a closed conformation of syntaxin1A. *J Cell Biol* 148:247–252, 2000
8. Riento K, Galli T, Jansson S, Ehnholm C, Lehtonen E, Olkkonen VM: Interaction of Munc-18-2 with syntaxin 3 controls the association of apical SNAREs in epithelial cells. *J Cell Sci* 111:2681–2688, 1998
9. Tamori Y, Kawanishi M, Niki T, Shinoda H, Araki S, Okazawa H, Kasuga M: Inhibition of insulin-induced GLUT4 translocation by Munc18c through interaction with syntaxin4 in 3T3–L1 adipocytes. *J Biol Chem* 273:19740–19746, 1998
10. Pevsner J: The role of Sec1p-related proteins in vesicle trafficking in the nerve terminal. *J Neurosci Res* 45:89–95, 1996
11. Katagiri H, Terasaki J, Murata T, Ishihara H, Ogihara T, Inukai K, Fukushima Y, Anai M, Kikuchi M, Miyazaki J, et al.: A novel isoform of syntaxin-binding protein homologous to yeast Sec1 expressed ubiquitously in mammalian cells. *J Biol Chem* 270:4963–4966, 1995
12. Pevsner J, Hsu SC, Scheller RH: n-Sec1: a neural-specific syntaxin-binding protein. *Proc Natl Acad Sci U S A* 91:1445–1449, 1994
13. Tellam JT, Macaulay SL, McIntosh S, Hewish DR, Ward CW, James DE: Characterization of Munc-18c and syntaxin-4 in 3T3–L1 adipocytes: putative role in insulin-dependent movement of GLUT-4. *J Biol Chem* 272: 6179–6186, 1997
14. Fujita Y, Shirataki H, Sakisaka T, Asakura T, Ohya T, Kotani H, Yokoyama S, Nishioka H, Matsuura Y, Mizoguchi A, Scheller RH, Takai Y: Tomosyn: a syntaxin-1-binding protein that forms a novel complex in the neurotransmitter release process. *Neuron* 20:905–915, 1998
15. Yokoyama S, Shirataki H, Sakisaka T, Takai Y: Three splicing variants of tomosyn and identification of their syntaxin-binding region. *Biochem Biophys Res Commun* 256:218–222, 1999
16. Groffen AJA, Jacobsen L, Schut D, Verhage M: Two distinct genes drive the expression of seven tomosyn isoforms in the mammalian brain, sharing a conserved structure with a unique variable domain. *J Neurochem* 92:554–568, 2005
17. Hatsuzawa K, Lang T, Fasshauer D, Bruns D, Jahn R: The R-SNARE motif of tomosyn forms SNARE core complexes with syntaxin 1 and SNAP-25 and down-regulates exocytosis. *J Biol Chem* 278:31159–31166, 2003
18. Masuda ES, Huang BC, Fisher JM, Luo Y, Scheller RH: Tomosyn binds t-SNARE proteins via a VAMP-like coiled coil. *Neuron* 21:479–480, 1998
19. Widberg CH, Bryant NJ, Girotti M, Rea S, James DE: Tomosyn interacts with the t-SNAREs syntaxin4 and SNAP23 and plays a role in insulin-stimulated GLUT4 translocation. *J Biol Chem* 278:35093–35101, 2003
20. Constable JRL, Graham ME, Morgan A, Burgoyne RD: Amisyn regulates exocytosis and fusion pore stability by both syntaxin-dependent and syntaxin-independent mechanisms. *J Biol Chem* 280:31615–31623, 2005
21. Yizhar O, Matti U, Melamed R, Hagalili Y, Bruns D, Rettig J, Ashery U: Tomosyn inhibits priming of large dense-cored vesicles in a calcium-dependent manner. *Proc Natl Acad Sci U S A* 101:2578–2583, 2004
22. Sakisaka T, Baba T, Tanaka S, Izumi G, Yasumi M, Takai Y: Regulation of SNAREs by tomosyn and ROCK: implication in extension and retraction of neurites. *J Cell Biol* 166:17–25, 2004
23. Dybbs M, Ngai J, Kaplan JM: Using microarrays to facilitate positional cloning: identification of tomosyn as an inhibitor of neurosecretion. *PloS Genetics* 1:6–16, 2005
24. Pobbati AV, Razeto A, Boddener M, Becker S, Fasshauer D: Structural basis for the inhibitory role of tomosyn in exocytosis. *J Biol Chem* 279:47192–47200, 2004
25. Zhang W, Efanov A, Yang SN, Fried G, Kolare S, Brown H, Zaitsev S, Berggren PO, Meister B: Munc-18 associates with syntaxin and serves as a negative regulator of exocytosis in the pancreatic β-cell. *J Biol Chem* 275:41521–41527, 2000

26. Lernmark Å: The preparation of, and studies on, free cell suspensions from mouse pancreatic islets. *Diabetologia* 10:431–438, 1974
27. Nilsson T, Arkhammar P, Hallberg A, Hellman B, Berggren PO: Characterization of the inositol 1,4,5-trisphosphate-induced Ca^{2+} release in pancreatic β-cells. *Biochem J* 248:329–336, 1987
28. Hellman B: Studies in obese-hyperglycemic mice. *Ann N Y Acad Sci* 131:541–558, 1965
29. Lilja L, Yang S-N, Webb D-L, Berggren L, Berggren P-O, Bark C: Cyclin-dependent kinase 5 promotes insulin exocytosis. *J Biol Chem* 276:34199–34205, 2001
30. Buchan AM, Sikora LK, Levy JG, McIntosh CH, Dyck I, Brown JC: An immunocytochemical investigation with monoclonal antibodies to somatostatin. *Histochemistry* 83:175–180, 1985
31. Merglen A, Theander S, Rubi B, Chaffard G, Wollheim CB, Maechler P: Glucose sensitivity and metabolism-secretion coupling studied during two-year continuous culture in INS-1E insulinoma cells. *Endocrinology* 145:667–678, 2004
32. Lilja L, Johansson JU, Gromada J, Mandic SA, Fried G, Berggren PO, Bark C: Cyclin-dependent kinase 5 associated with p39 promotes Munc18-1 phosphorylation and Ca^{2+}-dependent exocytosis. *J Biol Chem* 279:29534–29541, 2004
33. Martell AE, Smith RM: Amino Acids. Vol. 1. Plenum Press, New York, 1971
34. Martell AE, Smith RM. Amines. Vol. 2. Plenum Press, New York, 1971
35. Lehman K, Rossi G, Adamo JE, Brennwald P: Yeast homologues of tomosyn and lethal giant larvae function in exocytosis and are associated with the plasma membrane SNARE, Sec9. *J Cell Biol* 146:125–140, 1999
36. Baba T, Sakisaka T, Mochida S, Takai Y: PKA-catalyzed phosphorylation of tomosyn and its implication in Ca^{2+}-dependent exocytosis of neurotransmitter. *J Cell Biol* 170:1113–1125, 2005